Long-term drying shrinkage of self-compacting concrete: experimental and analytical investigations

J. Abdalhmid[a,b,] A.F. Ashour[b] and T. Sheehan[b]

University of Bradford, UK

[a] Corresponding Author, Civil Engineering Department, Tobruk University, Tobruk, Libya
Email: Jamilaabdalhmid2012@gmail.com
[b] School of Engineering, University of Bradford, UK.

Abstract

The present study investigated long-term drying shrinkage strains of self-compacting concrete (SCCs). For all SCCs mixes, Portland cement was replaced with 0-60% of fly ash (FA), fine and course aggregates were kept constant with 890 kg/m3 and 780 kg/m3, respectively. Two different water binder ratios of 0.44 and 0.33 were examined for both SCCs and normal concrete (NCs). Fresh properties of SCCs such as filling ability, passing ability, viscosity and resistance to segregation and hardened properties such as compressive and flexural strengths, water absorption and density of SCCs and NCs were also determined. Experimental results of drying shrinkage were compared to five existing models, namely the ACI 209R-92 model, BSEN-92 model, ACI 209R-92 (Huo) model, B3 model, and GL2000. To assess the quality of predictive models, the influence of various parameters (compressive strength, cement content, water content and relative humidity) effecting on the drying shrinkage strain as considered by the models are studied. The results showed that, using up to 60% of FA as cement replacement can produce SCC with a compressive strength as high as 30 MPa and low drying shrinkage strain. SCCs long-term drying shrinkage from 356 to 900 days was higher than NCs. ACI 209R-92 model provided a better prediction of drying shrinkage compared with the other models.

Keywords: Self-compacting concrete (SCC), Drying shrinkage strain, Fly ash, Drying Shrinkage models.

1 Introduction

Self–compacting concrete (SCC) has good deformability and high resistance to segregation which is easily placed and compacted under its self-weight, filling in heavily reinforced sections with little or no vibration. It is generally accepted that SCC was first developed at the University of Tokyo, Japan during the late 1980s (Okamura and Ouchi, 2003). Basically SCC consists of the same components as normal concrete (NC) (cement, water, aggregates, admixtures, and mineral additions), but the final composition of the mixture and its fresh characteristics are different. In comparison with NC, SCC mixtures are usually designed with high volumes of paste, large quantities of mineral fillers such as finely crushed limestone or fly ash and high range water reducing admixtures and the maximum size of the coarse aggregate is smaller.

All the special characteristics of SCC may have a significant influence on its shrinkage behaviour. Shrinkage of concrete is defined as the decrease of concrete volume with time after hardening of concrete in an unloaded specimen. This contraction is due to changes of moisture content of concrete. There are different types of concrete shrinkage; plastic shrinkage (due to loss of water by evaporation from concrete surface during the plastic state), chemical shrinkage (due to concrete hydration), autogenous shrinkage (due to self-desiccation after final setting), carbonation shrinkage (due to chemical reactions between hydrated cement and carbon dioxide (CO_2) present in the atmosphere) and drying shrinkage (due to the evaporation of internal water in hardened

concrete. Drying shrinkage strains (DS) is considered as a major concern for concrete deterioration, it produces tensile stress within concrete leading to cracking, which enables harmful materials to penetrate the concrete, affecting long term concrete durability.

Some discrepancy remains regarding the drying shrinkage strains of SCC (DSSCC) compared to drying shrinkage of normal concrete (DSNC). For example, Kim et al. (1998), Rols et al. (1999), Chan et al. (2003), Klug and Holschemacher (2003), Chopin et al. (2003), Turcry and Loukili (2003), Heirman and Vandewalle (2003), Turcry et al. (2006), Loser and Leemann (2009), Valcuende et al. (2012) and Bhirud and Sangle (2017) pointed out that SCC can exhibit higher shrinkage compared with NC. However, other investigators such as Persson (2001), Bouzoubaa and Lachemi (2001), Pons et al. (2003), Vieira and Bettencourt (2003), Poppe and De Schutter (2005), Seng and Shima (2005), Collepardi et al. (2005), Pierard et al. (2005) and Assié et al. (2007) concluded that the shrinkage strains of SCC are equivalent to those of NC with similar compressive resistance, and in some cases it was even found that the shrinkage of SCC was lower than NC (Proust and Pons, 2001, Heirman et al., 2007, Huynh et al., 2018).

The discrepancy between the experimental results of DSCC and DSNC could be related to the differences in concrete mixtures studied, testing conditions, and testing methods (Fernandez-Gomez and Landsberger, 2007). Moreover, most of the previous studies took into account only DS that was determined after a specific time of curing or immediately after demoulding, while other researchers considered DS that started from the setting time, including autogenous shrinkage. In this investigation, in order to compare between

DSSCC and DSNC magnitude the environmental conditions (relative humidity, temperature and curing type) and concrete condition (casting and testing) were kept same for SCCs and NCs and the measurements of drying shrinkage strain were taken immediately after demoulding.

This study was undertaken to investigate the properties of eight types of SCCs with different replacement ratios of fly ash (FA) for SCC mixes (20%, 40% and 60%) by weight of the binder, and two types of NCs in the fresh and hardened states. The mixes were prepared with two types of water-binder ratio (w/b) 0.33 and 0.44. The properties of the fresh state which included filling ability, passing ability and segregation resistance and the properties of the hardened state including compressive strength, flexural strength, water absorption, bulk density and drying shrinkage strains were measured in this study. The work was completed with a study of long-term DS. All of the results of SCCs are compared to those obtained with NCs. Prediction models proposed by international codes and other researchers, namely the ACI 209 R-92, ACI 209R-92 (Huo), BS EN-92, B3, and GL2000, have been used to assess the drying shrinkage prediction of SCCs and NC and compared with the experimental results.

2 Research significance

Drying shrinkage produces tensile stress within concrete leading to cracking, enabling harmful materials to penetrate the concrete, affecting economic factors of construction such as durability, serviceability and long term reliability. Different studies have been carried out covering drying shrinkage of self-compacting concrete (DSSCC). However, some discrepancy remains regarding

the drying shrinkage strain magnitudes of SCC compared to NC. Investigating the main parameters affecting the DSSCC and (DSNC) in the current study could explain that discrepancy and will increase the limited number of previous research studies on the drying shrinkage magnitude of SCC compared to that of NC. Measurements of drying shrinkage after demoulding have been monitored for more than two years.

The other objective of this paper is to compare the measured drying shrinkage strains with five drying shrinkage strain prediction models, namely the ACI209 R-92 model, ACI 209R-92 (Huo) model, BS EN-92 model, B3 model, and GL2000 model. The proper evaluation of DSSCC will provide construction materials engineers with a good understanding of the long term drying shrinkage behaviour of SCC and with the information required for the design process and production of high quality SCC.

3 Experimental program

3.1 Materials

The materials used in various experiments are given below.

Cement: Ordinary Portland cement (OPC), CEM I 52.5N complying with EN 197-1:2011 was used for all of the experimental work in this study. Physical properties and chemical compositions of the cement as provided by the supplier are given in **Table 1.**

Fly ash: Fly ash BS EN 450 -1, fineness category S, loss on ignition category B, grey colour was used as a partial replacement of Portland cement. Physical properties and chemical compositions of the fly ash as provided by the supplier are presented in **Table 1.**

Table 1 Physical properties and chemical compositions of cement and fly

Cement replacement materials	Cement (CEMI 52.5 N)	Fly ash (450-S)
Physical properties		
Specific gravity	3.15	2.15
Blaine specific surface area, m^3/kg	400	461
28 days Compressive strength, (MPa)	60.0	-
Initial setting time (Mins)	150	-
Soundness, expansion (mm)	1	< 0.1
Chemical composition, %		
S_iO_2	20.10	51
AL_2O_3	5.04	29
Fe_2O_3	2.28	7.6
C_aO	36.24	2.5
M_qO	2.50	1.5
SO_3	3.39	0.9
K_2O	0.62	2.36
$N_{a2}O$	0.28	-
Cl	0.05	< 0.05
LOI	2.87	1.6

Admixtures: A high range water reducing admixture (HRWRA) superplasticizer (SP) complying with BS EN 934-2:2001 was employed to achieve a suitable workability for SCC mixes. A shrinkage reducing admixture (SRA 895) was used to reduce significantly the drying shrinkage strains of SCCs. Physical and chemical properties of SP and RSA provided by the supplier are given in Table **2.**

Table 2 Physical and chemical properties of SP and SRA

Properties	**Superplasticizer (SP)**	**Shrinkage reducing admixture (SRA)**
Name	Glenimum C315	MasterLife SRA 895
Form	liquid	liquid
Colour	yellowish	colorless
pH value	5 - 8	-
Specific gravity	1.10 ± 0.03	1.01 ± 0.02
Dosage range	0.10-1.10% of binder content	0.50-2.0 % of binder content

Aggregates: All SCC and NC concrete mixtures were prepared with a crushed coarse limestone aggregate (C_{agg}) with a maximum size of 10 mm and a local natural sand (F_{agg}) with a maximum aggregate size of 4.75 mm. For each aggregate, the relative density on saturated dry basis and dry, water absorption (% of dry mass), and apparent specific gravity were determined in accordance with ASTM C127-15 and bulk density of aggregates were measured in accordance to ASTM C29/C29M-15. The determination of the percentage of evaporable moisture in a sample of aggregates were tested according to ASTM C566-15. All materials were collected and stored in the laboratory to ensure their constant absorption characteristics and keep the same environmental conditions throughout the test program. Results obtained of physical properties of the aggregates are summarized in **Table 3.** The particle size distributions of coarse and fine aggregates were within the limits set by ASTM C33. Grading of the aggregates with the ASTM limits are plotted in **Figure 1.**

Table 3 Physical properties of coarse and fine aggregates

Property of aggregate	Coarse aggregate	Fine aggregate
Relative density (SSD)	2.55	2.51
Relative density (Dry)	2.58	2.54
Absorption (% of dry mass)	0.42	0.60
Apparent specific gravity	2.61	2.60
Water content (kg/m^3)	0.61	1.47
Bulk density (kg/m^3)	1500	1400
Fineness modulus	7.20	2.90

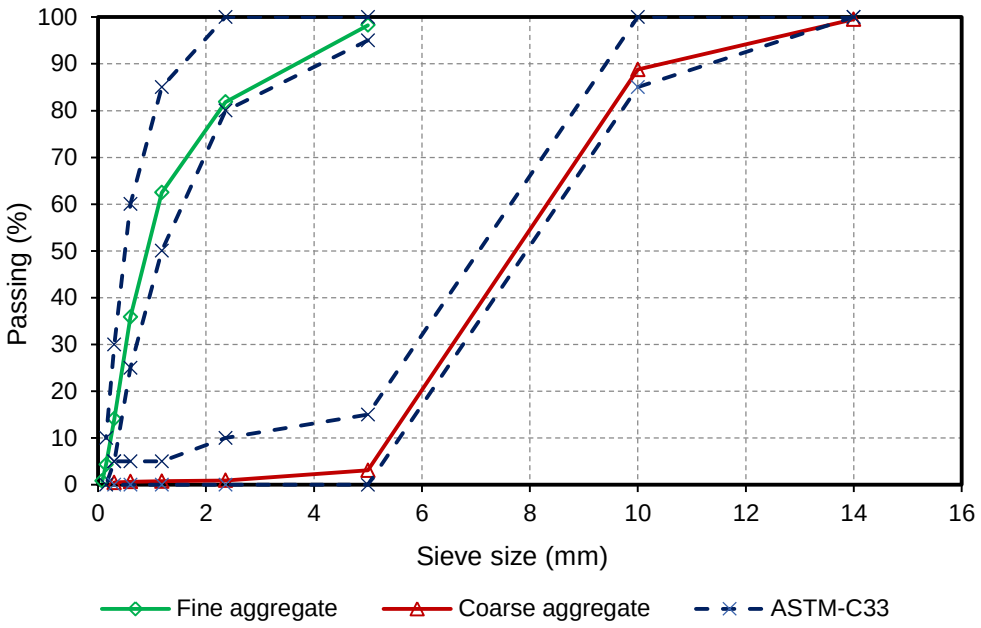

Figure 1 Grading of coarse and fine aggregates

3.2 Mix design proportions

A total of 8 SCCs mixtures were designed following the SCC mix design method proposed by Su et al. (2001) with some modification in mix proportion. Two NCs mixtures as control mixes using the weight-batching method according to the Building Research Establishment were also considered (Teychenné et al., 1975). All concrete mixtures were designed at two water-binder ratios (w/b) of 0.44 and 0.33. The replacement ratio of fly ash (FA) for SCCs mixes were 20%, 40% and 60% by weight of the binder. For all SCCs mixes packing factor (PF), air content (A %) and volume ratio of fine aggregates to total aggregates are assumed 1.16, 1.5 and 53%, respectively. Mixture proportions of the eight SCCs (SCC-0.44, SCC-0.33, SCC-0.44-20, SCC-0.4440, SCC-0.44-60, SCC-0.33-20, SCC-0.33-40 and SCC-0.33-60) and two NCs (NC-0.44 and NC-0.33) mixtures are summarized in **Table 4.**

Table 4 Proportions of concrete mixtures per m^3

Mix ID	w/b ratio	B	C	FA	W (Kg)	C_{agg}	F_{agg}	SP	SRA (%)	A
NC-0.44	0.44	466	466	0	205	924	755	0	0	1.5
NC-0.33	0.33	622	622	0	205	883	640	0	0	1.5
SCC-0.44	0.44	450	450	0	198	780	890	1	0	1.5
SCC-0.33	0.33	550	550	0	180	780	890	1	0	1.5
SCC-0.44-20	0.44	450	360	90	198	780	890	1	1	1.5
SCC-0.33-20	0.33	550	440	110	180	780	890	1	1	1.5
SCC-0.44-40	0.44	450	270	180	198	780	890	1	1	1.5
SCC-0.33-40	0.33	550	330	220	180	780	890	1	1	1.5
SCC-0.44-60	0.44	450	180	270	198	780	890	1	1	1.5
SCC-0.33-60	0.33	550	220	330	180	780	890	1	1	1.5

3.3 Mixing and specimens preparation

All concrete mixtures were prepared in 0.08 m^3 batches using a drum mixer. For SCC mixtures the ingredients were poured into the laboratory counter mixer in the following order; coarse aggregate (C_{agg}), fine aggregate (F_{agg}), cement (C), fly ash (FA), water mixed with admixtures (HRWRA and SRA); the same procedure is followed for the NC mixtures without fly ash and admixtures. This procedure was adopted for all of the mixes in order to minimize the risk of a possible disparity between the homogeneity of each mix. Dry ingredients (aggregates and binder (B)) were mixed for 3 minutes, then water (with HRWRA and SRA for SCC mixtures only) was gradually added in 15 seconds and the mixing continued for 3 minutes followed by a 2 minute final mix. The top of the mixer was covered to prevent evaporation during the mix period in accordance with ASTM C192/C 192M-14. For each concrete mixture, different sizes (cubes and prisms) of concrete specimens were prepared and cast in steel moulds for testing water absorption, density, compressive strength, flexural strength and drying shrinkage strains. All of the specimens (cubes and prisms) were not subjected to any compaction other than their own self weights except for NC

specimens. After casting, the specimens were kept covered in a controlled chamber at 20±2^{0}C for 24 h until demoulding and then cured as presented in the following sections.

3.4 Testing procedure

3.4.1 Fresh properties tests

Self-compacting concrete is characterized by viscosity, filling ability, passing ability and resistance to segregation and it is important to keep these characteristics during transport and placing. The viscosity of SCC was evaluated using the slump flow test, the flow spread and T_{500} time representing horizontal free flow of the mass of concrete after release of a standard slump cone. The assessment of SCC filling ability which represent ability of fresh concrete to distort and flow under its own weight without vibration or extra assistance into the formwork was measured used V-funnel test.

The passing ability of SCC determines how well the concrete can flow through confined and constricted spaces and narrow openings. It was examined using the J-ring test. The sieve stability test (screen stability test) for segregation resistance was used to measure static segregation of SCCs. All SCC fresh properties were determined according to the European Guidelines for SCC (BIBM and ERMCO, 2005). To measure the workability of NC, slump test accordance to ASTM C143/ C143-13 was used.

3.4.2 Mechanical properties tests

Compressive strength was measured by testing three cube specimens with 100×100×100 mm size in accordance with BS EN12390-3:2009. The specimens were cast, left covered with plastic sheet in a controlled room at 20±

2 ^{o}C for 24h until demoulding. Thereafter, specimens placed in water for curing time until tested at 7, 28 and 91 days using the compressive strength testing machine at a constant rate of 0.2 MPa/s with a maximum load capacity 3000-KN and the results were obtained as the average.

Flexural strength was measured by testing two prism specimens with 100×100×500 mm size in accordance with ASTM C78/78M-13. The test was performed using testing machine with a constant rate of 0.05MPa/s until fracture. The curing condition for prism specimens were the same as those for the compressive strength specimens.

3.4.3 Water absorption and density tests

Water absorption test in accordance with BS 1881-122 was used to determine the amount of water absorbed which indicates the degree of porosity of concrete. The determination of concrete density was evaluate in accordance with BS 1881-114. Specimens with 100×100×100 mm cube size placed in dry oven at 100±5 °C for 24 h. After removing each specimen from the oven, it allow to cool in dry air to a temperature of 20 to 25°C and the average weight of oven dry specimens was recorded and immediately after drying and cooling, the specimens completely immersed in water at 21°C for 24 h. The specimens then were turned to saturated surface dry by removing water from the surface using a moist cloth. Then the average weight of specimens was taken. The water absorption as a percentage was calculated as the ratio of water mass absorbed to that of dry mass of specimen. The density of concrete was determined as the ratio of dry mass to the volume mas of specimen and expressed as a percentage.

3.4.4 Drying shrinkage strains test

The determination of drying shrinkage strain was conducted on the prisms of 100×100×300 mm size. Specimens were cast in three layers and covered with a plastic sheet to prevent moisture loss then demoulded after 24 ± 2 hr and demec points were fixed on the top surface of the specimens by using an epoxy adhesive. The variation in length between these points when the specimens were exposed to shrinkage conditions was measured using a dial gage extensometer that was 220 mm long with an accuracy of 0.001 mm/division. The drying shrinkage strain measurements were monitored for the long term at 4, 7, 14, 21, 28, 50, 91, 112, 224, 365, 500, 730, 900 and 1000 days after an initial reading at 24 hours after demoulding. At each measurement age, drying shrinkage of a specimen was calculated for the same side and direction as the other ages to reduce the error in the readings. During testing all specimens were left to air cure in a controlled room at 23 ± 2°C with a relative humidity of 50± 5 %. The tests are carried out following the ASTM C157/13 for determination of length change in hardened cement mortar and concrete. The drying shrinkage strains were calculated using the formula below;

$$\varepsilon_{sh} = \frac{CRD - initial\ CRD}{G} \qquad (1)$$

where $\boldsymbol{\varepsilon_{sh}}$ is the drying shrinkage strain of specimen (mm/mm), CRD is the difference between the comparator reading of the specimen (mm) and the reference bar at any age, initial CRD is the difference between the comparator reading of the specimen and the reference bar at first reading, G is the gage length (220 mm).

4 Experimental results and discussion

4.1 Fresh properties

The results of fresh properties of SCCs were evaluated by the slump flow test (slump flow diameter and T_{500mm}), J-ring test (flow diameter and T_{500mm}), V-funnel (time taken by concrete to completely exit through the funnel) and sieve stability test (calculated as the proportion (as%) of the sample passing through the sieve) according to EFNARC (BIBM and ERMCO, 2005). The values of the fresh properties for all SCC and NC mixes obtained in this work are shown in **Table 5.**

The slump of NC mixes with w/b ratios 0.44 and 0.33 were 110mm and 63mm, respectively. All SCC mixes in this study exhibited satisfactory workability, in that the flow spread (diameters) for all mixes was in a range of 655 – 808 mm and the time which the concrete took to exit the v-funnel was between 6.5 – 11 sec. A slump flow of 600± 50 – 850 mm and a funnel time of 5 – 15 sec were required (BIBM and ERMCO, 2005). For a J-ring value below 500 mm, the concrete might have had insufficient flow to pass through highly congested reinforcement (Nagataki and Fujiwara, 1995). The SCC mixes in this work were acceptable with J-ring values between 560- 795 mm. The segregation ratio for all mixes ranged between 10– 19 %. When the segregation ratio stays ≤ 23% of the weight of the sample, the resistance to segregation ability is considered acceptable (BIBM and ERMCO, 2005). A comparison between workability experimental results and specifications of European guidelines is plotted in **Figure 1.** As observed throughout this experimental work, workability SCC mixes containing FA were achieved with its fresh properties required at a constant water to binder ratio. Therefore, using FA will reduce water demand for

a given workability. SCCs made with w/b ratio 0.44 were more workable than those made with w/b ratio 0.33. Most of the mixtures showed good homogeneity and cohesion. To analyse the workability results of SCCs, the concept of workability is presented in Figure **3** using boxes, where mixes within the area are acceptable SCC (Esquinas et al., 2018). The mixes inside the box in the section named “Proper SCC area" are regarded as suitable and acceptable SCCs, whereas the other mixes which located in the area named “marginal area” are acceptable as SCCs with a slight segregation could occur. None of the mixes in the present investigation were observed in unacceptable SCC area.

Table 5 Workability results of NCs and SCCs

Mix ID	Slump	Slump flow	J-Ring					V-funnel	Segregation		
		T_{500}	d1	d2	T_{500}	d1	d2				
	(mm)	(sec)	(mm)	(mm)	(sec)	(mm)	(mm)	sec	W_p	W_c	%
NC-0.44	110	.	.	.	.	.	.	.	.	.	.
NC-0.33	63	.	.	.	.	.	.	.	.	.	.
SCC-0.44	.	1.78	760	780	3.19	700	720	9.1	501	4855	10.3
SCC-0.33	.	5.00	660	650	7.00	560	590	11	556	4710	11.8
SCC-0.44-20	.	2.70	790	780	3.00	770	760	8.7	593	4772	12.3
SCC-0.33-20	.	3.44	810	770	5.10	770	830	10	816	4894	14
SCC-0.44-40	.	2.97	670	630	2.13	540	580	7.3	945	4800	14.8
SCC-0.33-40	.	3.20	770	820	4.13	790	770	9.3	1088	4808	16
SCC-0.44-60	.	2.50	710	740	1.6	580	570	6.5	488	4815	17
SCC-0.33-60	.	4.00	780	835	3.61	805	785	8.1	943	4824	19

Wp; weight of passed concrete and Wc ; weight of net concrete

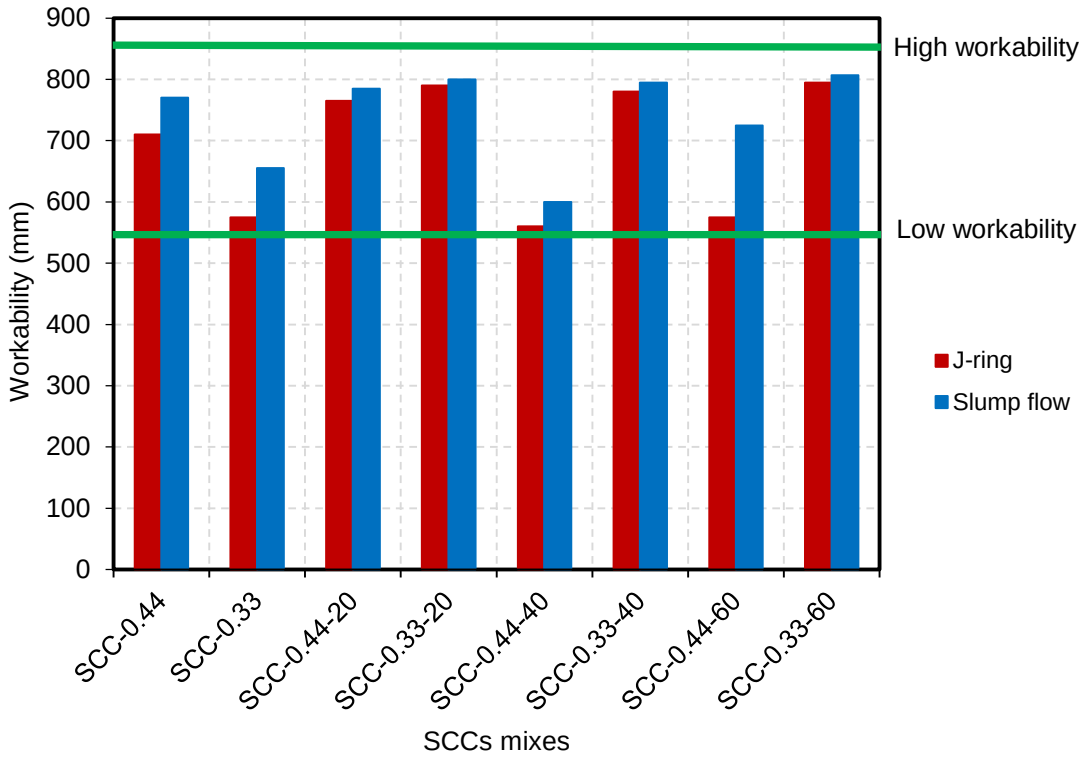

Figure 2 Slump flow and J-ring results

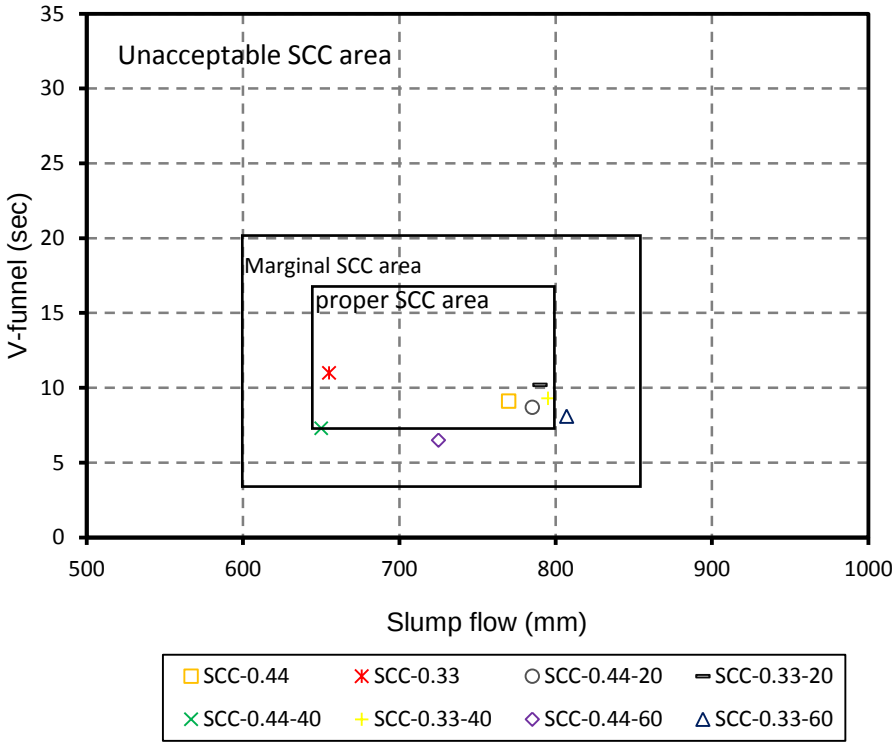

Figure 3 Workability boxes of SCC mixes

4.2 Compressive strength

The compressive strengths of eight SCC mixes and two NC mixes are shown in **Table 6.** Normal concretes, NC-0.44 and NC-0.33 have achieved compressive strengths of 48.65 MPa and 63.65 MPa at 28 days, respectively compared with self-compacting concretes, SCC-0.44 and SCC-0.33 which have reached 55.10MPa and 70.13 MPa at 28 days, respectively. It is clear that for the same water - binder ratio SCCs have higher compressive strength than NCs. This mainly attributed to the improved interface transition zone between the aggregate and hardened paste due to the absence of vibration of SCCs.

It is observed that the compressive strength of SCCs decreased with an increase in the percentage of FA as illustrated in **Figure 3** and **Figure 4** This reduction is normally anticipated and is mostly due to the fact that FA needs more time to form the sodium alumino-silicate hydrate (N-A-S-H) gels to build up the mechanical properties (Ismail et al., 2014). The same conclusions have been drawn by Khatib (2008) and Bouzoubaa and Lachemi (2001).

All SCCs mixes have achieved acceptable 28-day compressive strengths of about 30 MPa. However, SCCs mixes with 60% FA and a w/b ratio of 0.44 had a 28-day compressive strength of 21.63 MPa. Moreover, a long term compressive strength at 91 days of above 30 MPa was achieved for SCC mixes containing up to 60% FA as cement replacement (SCC-0.44-60 and SCC-0.33-60). As expected, the compressive strength increased as the w/b ratio decreased at all test ages.

Table 6 Compressive and flexural strength of NCs and SCCs

Mix ID	Compressive strength (MPa)			Flexural strength (MPa)
	7(days)	28(days)	91(days)	91(days)
NC-0.44	43.2	48.65	54.09	4.66
NC-0.33	50.90	63.47	70.25	5.85
SCC-0.44	46	55.1	62.77	5.04
SCC-0.33	59.7	70.13	77.51	6.18
SCC-0.44-20	37.42	45.28	52.12	5.37
SCC-0.33-20	42.13	53.81	66	6.57
SCC-0.44-40	19.9	32.65	36.62	4.56
SCC-0.33-40	39.5	42.25	61.83	5.90
SCC-0.44-60	9.7	21.63	31.65	3.17
SCC-0.33-60	19.9	31.56	43.51	4.07

4.3 Flexural strength

All mixes results of flexural strength are shown in **Table 6.** A slight increase was observed for flexural strength of SCCs from 5.07 MPa to 5.37 MPa with a w/b ratio of 0.44 and from 6.18 MPa to 6.57 MPa with a w/b ratio of 0.33 containing 0% FA and 20% FA, respectively. However, by increasing FA from 40% to 60% for SCCs with both w/b ratios (0.44 and 0.33), the flexural strength decreased. A similar reduction in flexural strength of SCCs containing FA has been observed by Iqbal et al. (2017). This reduction of flexural strength of SCCs may be justified on the basis that the SCC compressive strength decreased which has a direct relationship with flexural strength of concrete. The NC flexural strengths were 4.66 MPa and 5.85 MPa for NCs with w/b ratios of 0.44 and 0.33, respectively. This relationship is graphically represented in **Figure 6**, from which this behaviour can be clearly observed.

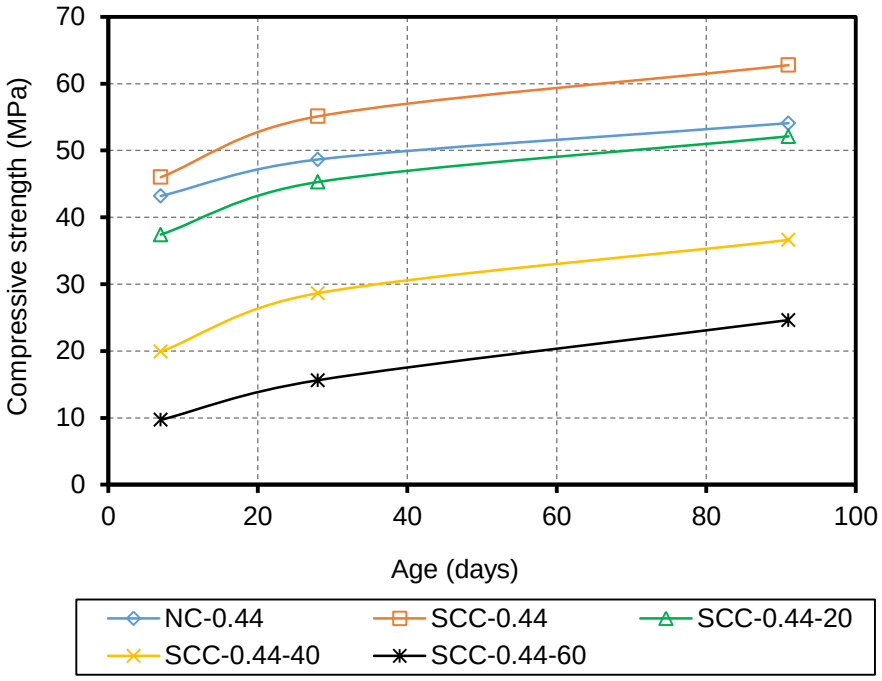

Figure 4 Effect of fly ash % on compressive strength for mixes with w/b ratio 0.44

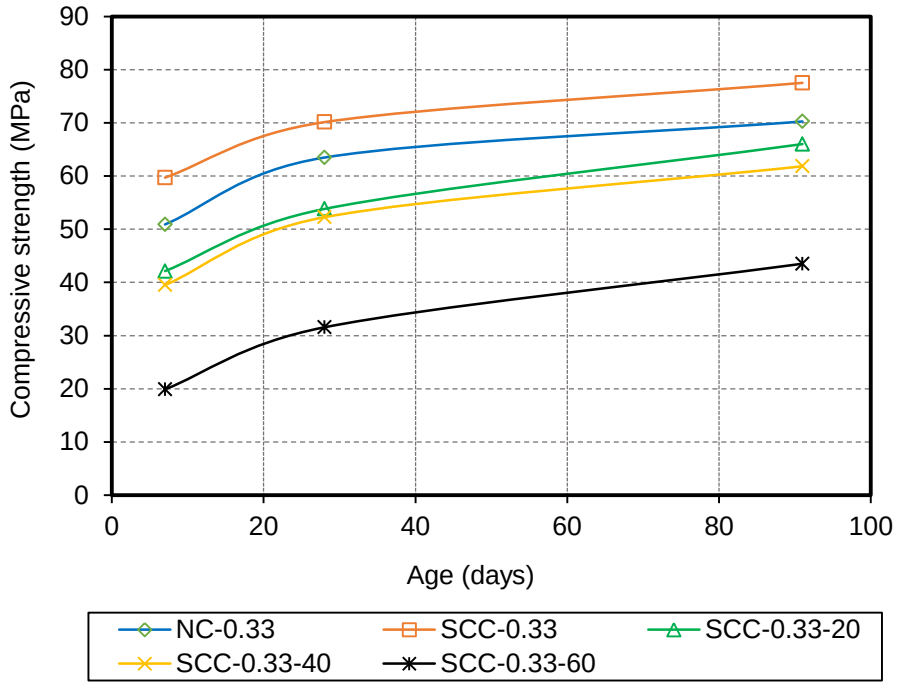

Figure 5 Effect of fly ash % on compressive strength for mixes with w/b ratio 0.33.

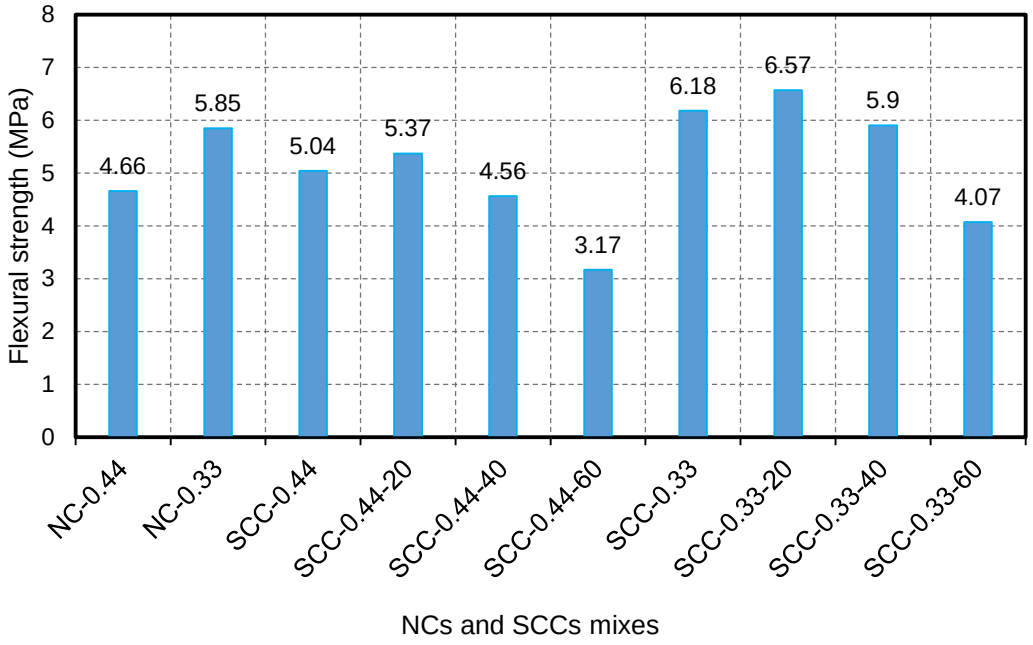

Figure 6 91-day flexural strength for NCs and SCCs mixes with w/c ratios 0.44 and 0.33

4.4 Bulk density

Bulk density for NCs and SCCs mixes for different w/b ratios are presented in **Table 7**. Each value of bulk density represents the average of three samples. The density slightly increased as the w/b ratio decreased from 0.44 to 0.33 for both NCs and SCCs which can be attributed to a reduction in the water content from 198 to 180 kg/m^3. Furthermore, at the same w/b ratio, the density of SCC showed a systematic reduction as FA increased due to the lower density of FA compared with ordinary Portland cement (OPC). Even though SCC proportions are different to NCs, a slight difference in density of SCCs compared to NCs has been observed in this study, agreeing with the findings of Khatib (2005), indicating the good self-compaction of SCCs.

4.5 Water absorption

Water absorption is generally used as a significant factor for quantifying the durability of cementitious systems. The influence of various degrees of FA content on water absorption for NCs and SCCs is illustrated in **Figure 7.** It can be noticed that there is an increase in water absorption for SCCs with increasing FA content. SCC mixes showed lower absorption compared to NC mixes. This is an indicator of good compaction achieved by the concrete self-weight. Due to the increase of workability of SCCs containing fly ash, the compaction is expected to be better All SCCs and NCs mixes having w/b ratios 0.33 showed lower water absorption than those made with w/b ratios 0.44 this could be attributed to their capillary and pore networks are somewhat disconnected, which restrains the water penetration depth. It is observed that the water absorption for all mixes varied between 4.6% and 8.8%. All concrete mixes had low absorption characteristics (less than 10%) which is in good agreement with the results reported by Siddique (2013).

Table 7 Bulk density of NCs and SCCs

Mix ID	FA (%)	Bulk density (kg/m^3)
NC-0.44	0	2230
NC-0.33	0	2238
SCC-0.44	0	2227
SCC-0.33	0	2241
SCC-0.44-20	20	2217
SCC-0.33-20	20	2236
SCC-0.44-40	40	2129
SCC-0.33-40	40	2178
SCC-0.44-60	60	2108
SCC-0.33-60	60	2141

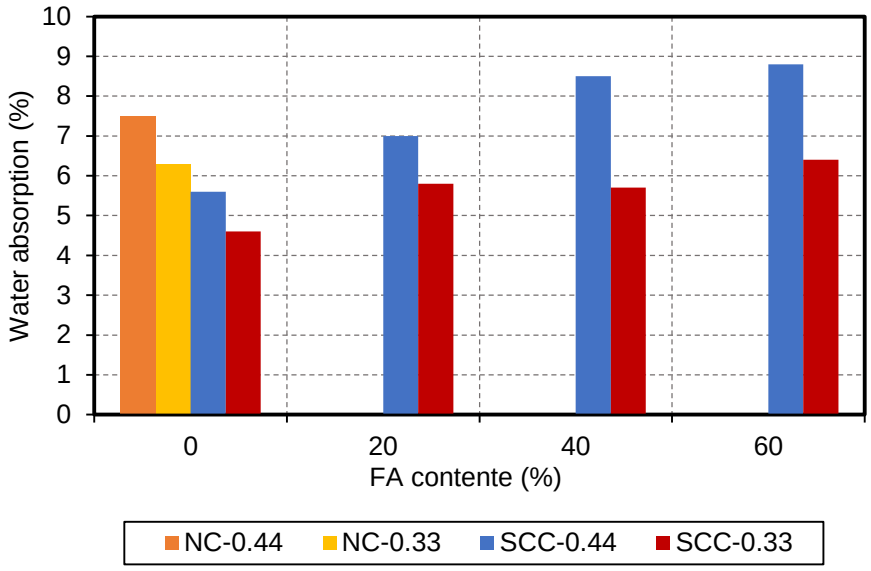

Figure 7 Effect of FA content on water absorption of NC and SCC mixes.

4.6 Drying shrinkage strains

Long term drying shrinkage strains for NCs and SCCs are summarized in **Table 8**. Drying shrinkage strain is considered as an important durability property, controlling the deterioration of concrete structures. The dying shrinkage strains for NCs and SCCs at 1000 days range between 316 and 695 microstrain. SCCs exhibited 10 to 15 % higher drying shrinkage strains compared to NCs for the same w/b ratio at different ages of drying. The effect of FA content on drying shrinkage strains and the variations with time for NCs and SCCs made with different w/b ratios (0.44 and 0.33) are illustrated in **Figure 8** and **Figure 9.** It is observed that the DSNC and DSSCC were slightly similar at the very early ages, whereas there was a considerable change in the long-term. It can be seen in **Figure 8** and **Figure 9** that the effect of replacing the cement by FA was to reduce the drying shrinkage strains remarkably at 40% and 60% FA replacement, but for all of the compositions the drying shrinkage strain increased with the increase of w/b ratio. At high FA content used in this study

(60%), the long term drying shrinkage strain (at 1000 days age) for SCCs was reduced to 49 % compared with the SCCs without FA which was consistent with the finding of Khatib (2005). The drying shrinkage of concrete depends on three controlling factors; w/b ratio, the volume of paste in concrete and the rate of hydration. In this study each of the five mixes had the same w/b ratio and paste volume. However, cement replacement by fly ash reduced the lime content from the mix as FA has a significantly low lime content in this study (2.5%). Due to the reduction of lime content, the rate of hydration of concrete reduced. As a result, fly ash concrete exhibited a lower degree of drying shrinkage compared to conventional concrete (Siddique, 2004, Saha and Sarker, 2017). It is clear that, the majority of concrete drying shrinkage strain occurred in the first three months. Afterwards, the long term drying shrinkage strain up to 1000 days was steady for all mixes.

Table 8 Drying shrinkage strains for various ages (microstrain).

	Age (days)						
Mix ID	28	50	112	365	500	900	1000
NC-0.44	388	475	565	583	595	625	632
NC-0.33	350	400	521	555	562	578	586
SCC-0.44	425	500	600	632	645	681	695
SCC-0.33	400	456	575	649	661	676	682
SCC-0.44-20	365	452	525	541	555	576	585
SCC-0.33-20	330	405	450	541	553	605	608
SCC-0.44-40	238	286	325	354	363	374	383
SCC-0.33-40	200	275	322	356	362	381	388
SCC-0.44-60	194	251	275	301	321	329	341
SCC-0.33-60	161	231	265	285	296	306	316

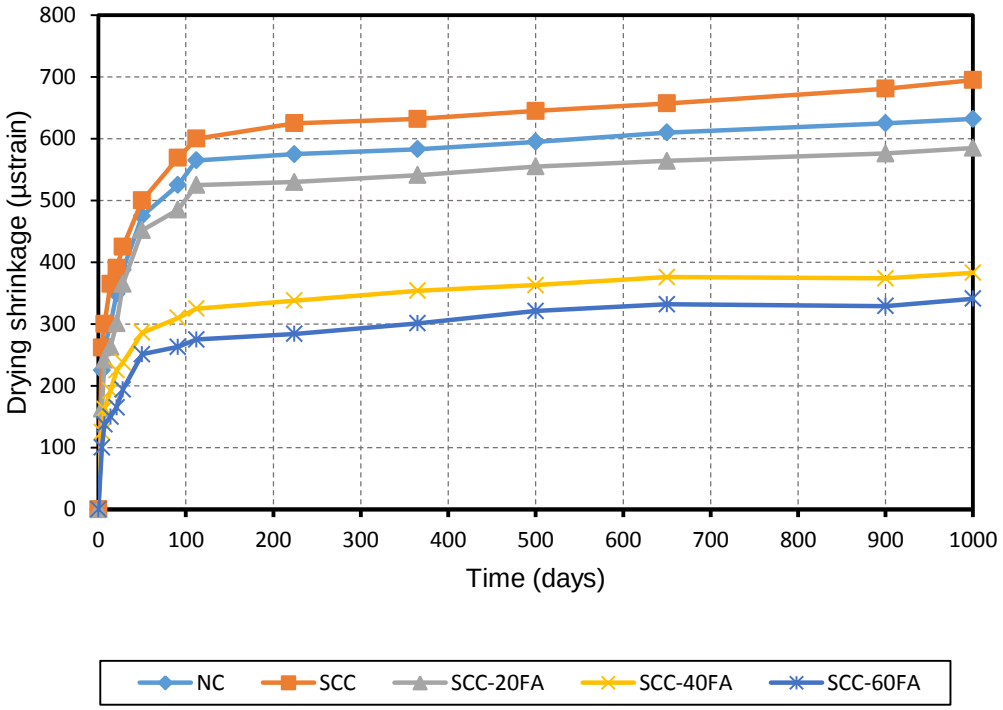

Figure 8 Effect of FA content on drying shrinkage strain for NCs and SCCs mixes with w/b ratio 0.44 at different ages

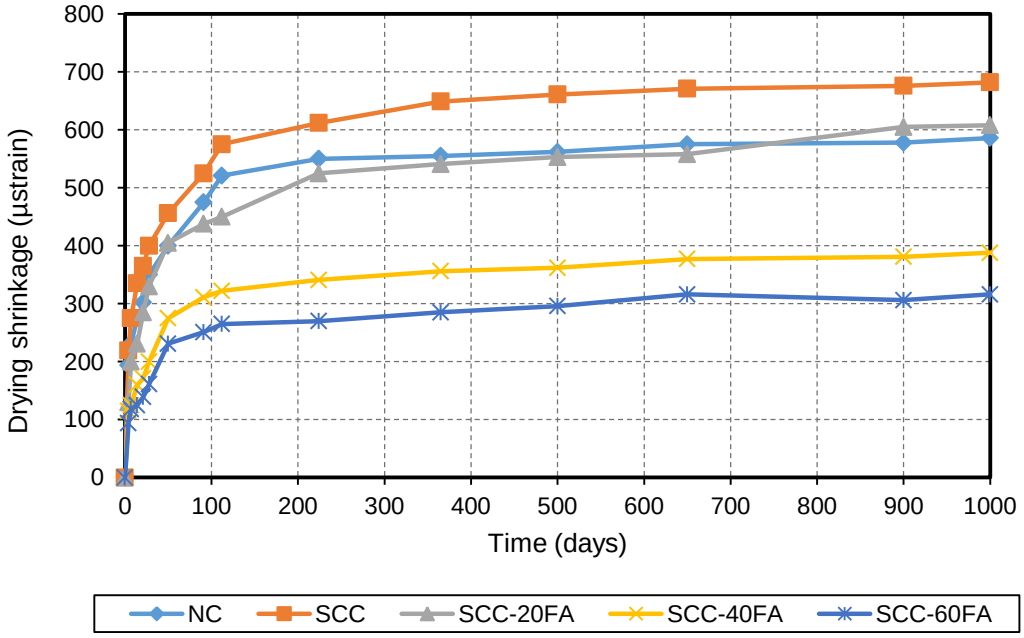

Figure 9 Effect of FA content on drying shrinkage strain for NCs and SCCs mixes with w/b ratio 0.33 at different ages

Figure 10 illustrates the relationship between FA content and drying shrinkage strain. There is a linear relation between FA content and drying shrinkage strain with R^2 = 0.951 and 0.950 for the two w/b ratios 0.44 and 0.33, respectively indicating a strong correlation for both w/b ratios. Khatib (2008) reported a linear relationship between drying shrinkage at 56 days against FA content of R^2 = 0.96 with a reduction in drying shrinkage by increasing FA content.

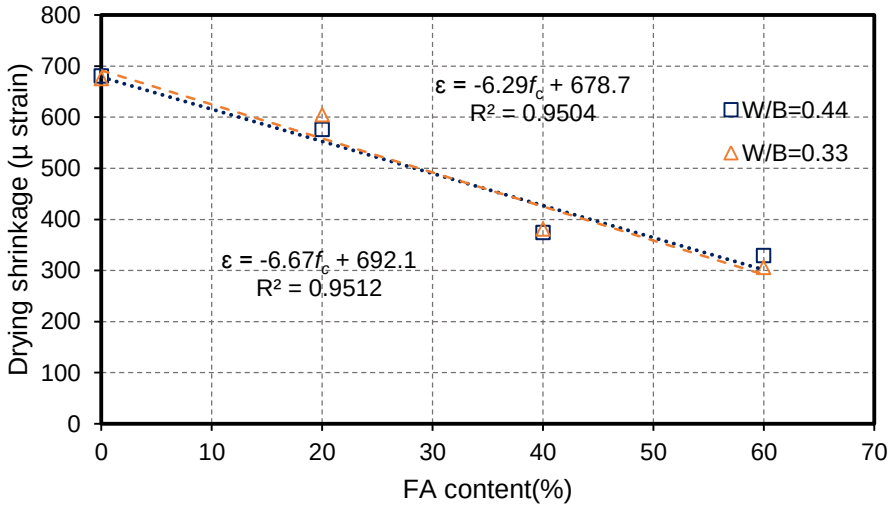

Figure 10 Relation between FA content and drying shrinkage at 1000 days for different w/b ratios.

Figure 11 correlates the drying shrinkage at 1000 days with the compressive strength at 91 days. It is clear that SCCs with a w/b ratio of 0.44 showed greater drying shrinkage strains than those with a w/b ratio of 0.33. At the same time SCCs with a w/b ratio of 0.33 which had higher compressive strengths exhibited reductions in the drying shrinkage. SCCs with the same w/b ratio displayed an increase in compressive strength when drying shrinkage increased and a linear relationship was obtained with R^2 = 0.975 and 0.866 for w/b ratios of 0.44 and 0.33 respectively, indicating a good correlation. As it is already known, by

increasing the w/b ratio, the compressive strength decreased. Consequently, drying shrinkage increased. The opposite trend was achieved in this study for which was similar to previous studies (Persson, 2001, Khatib, 2008) due to the presence of FA content which caused reductions in both compressive strength and drying shrinkage.

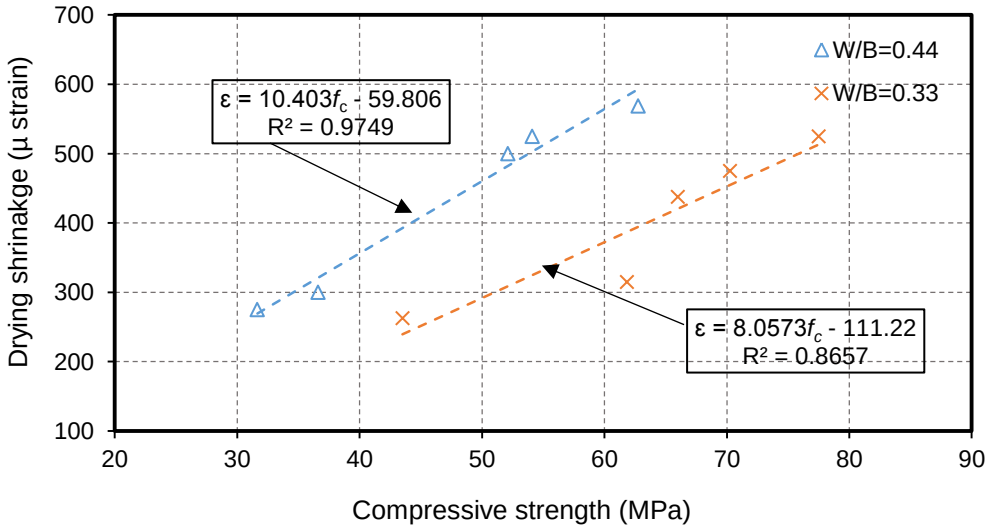

Figure 11 Relation between compressive strength and drying shrinkage at 1000 days for different w/b ratios.

5 Assessment of drying shrinkage strains prediction models

There are several empirical models that have been developed over several years to improve the accuracy of shrinkage strains prediction of concrete. These models vary in complexity, precision, and parameters necessary for the calculations. The prediction models selected for comparison in this study are the American Concrete Institute Committee (ACI 209R-92) model, the Eurocode 2 (BS EN- 92) model, the model modified by Huo (ACI 209R-92 (Huo), the model developed by Bazant and Baweja (B3) and Gradner and Lockman model (GL2000). The characteristics of these models are described briefly in **Table 7.**

To assess the quality of predictive models, the influence of various parameters on the drying shrinkage strain as predicted by various models are studied. Range of parameters for each model was used to assess the models Limitations of variables considered for each model are listed in **Table 8.** The main parameters considered in this study were compressive strength, cement content, water content and relative humidity.

Table 9 Summary of drying shrinkage models

Models	Equations
ACI 209R-92	Moist cured $\varepsilon_{sh}\ (t-t_c) = \frac{(t-t_c)}{35+(t-t_c)}\ \varepsilon_{sh\,u}$ $\varepsilon_{sh\,u}$= 780 γ_{sh} × 10^{-6} (mm/mm) Steam cured $\varepsilon_{sh}\ (t-t_c) = \frac{(t-t_c)}{55+(t-t_c)}\ \varepsilon_{sh\,u}$ γ_{sh}= $\gamma_{sh,tc}\gamma_{sh,RH}\gamma_{sh,vs}\gamma_{sh,s}\gamma_{sh,\psi}\gamma_{sh,c}\gamma_{sh,\alpha}$
ACI 209R-92 (Huo)	$\varepsilon_{sh}\ (t-t_c) = \frac{(t-t_c)}{(45-0.3625\,f'_c+(t-t_c)}\ \varepsilon_{sh\,\mu}$ $\varepsilon_{sh\,u}$= 780 γ_{sh} × 10^-6 (mm/mm) γ_{sh}= $\gamma_{sh,tc}\gamma_{sh,RH}\gamma_{sh,vs}\gamma_{sh,s}\gamma_{sh,\psi}\gamma_{sh,c}\gamma_{sh,\alpha}\gamma_{sh,S}$
BS EN-92	$\varepsilon_{cd}(t) = \beta_{ds}\,(t,t_s)\,k_h\ \varepsilon_{cd,0}$ $\beta_{ds} = \frac{t-t_c}{(t-t_c)+0.04\sqrt{h_0{}^3}}$ $\varepsilon_{cd,0} = 0.85\left[(220+110.\propto_{ds1}).\exp(-\propto_{ds2}.\frac{f_{cm}}{f_{cm0}}\right].10^{-6}.\beta_{RH}$ $\beta_{RH} = 1.55\left[1-\left(\frac{RH}{RH_0}^3\right)\right]$
GL2000	$\varepsilon_{sh}(t) = \varepsilon_{shu}\ \beta(h)\,\beta\,(t)$ $\beta(h) = (1-1.18h^4)$ $\beta(t) = \left[\frac{t-t_c}{t-t_c+0.12\times(\frac{V}{S})^2}\right]^{0.5}$ $\varepsilon_{shu} = 900\times K\times\left[\frac{30}{f_{cm28}}\right]^{1/2}\times 10^{-6}$
B3	$\varepsilon_{sh}(t) = \varepsilon_{shu}\,k_h\,S(t)$ $S(t) = tanh\sqrt{\frac{t-t_c}{\tau_{sh}}}$ τ_{sh}= $4.9D^2$ $\varepsilon_{shu} = \alpha 1\alpha 2[0.019w^{2.1}\,(f'_c)^{-0.28}+270]$
Parameters	t; time of concrete at drying (days), t_c; time of initial curing (days), $\varepsilon_{sh\,u}$; ultimate shrinkage strain (mm/mm), γ_{sh}; cumulative of correction factors, $\gamma_{sh,tc}, \gamma_{sh,RH}, \gamma_{sh,vs}, \gamma_{sh,s}, \gamma_{sh,\psi}, \gamma_{sh,c}, \gamma_{sh,\alpha}, \gamma_{sh,f'_c}$;coefficients of curing time, relative humidity, volume to surface specimen, slump, ratio of fine to total aggregate, cement content, air content, 28 days compressive strength of concrete, respectively. k_h ; relative humidity coefficient, D; cross section thickness of concrete, α_1; cement type coefficient, α_2; curing type coefficient, α_{ds}; cement type coefficient, f_{cm}; mean compressive strength.

Table 10 Variables range for each model

Parameters	ACI209R-92	BSEN-92	ACI209R (Huo)	GL2000	B3
Compressive strength (MPa)	-	20-100	60-80	16-82	17-70
Cement content (kg/m^3)	279-446	-	400-445	160-719	160-720
Water content (kg/m^3)	-	-	-	-	60-600
Relative humidity (%)	40-100	40-100	40-100	20-100	40-100

5.1 Effect of compressive strength on drying shrinkage using various models

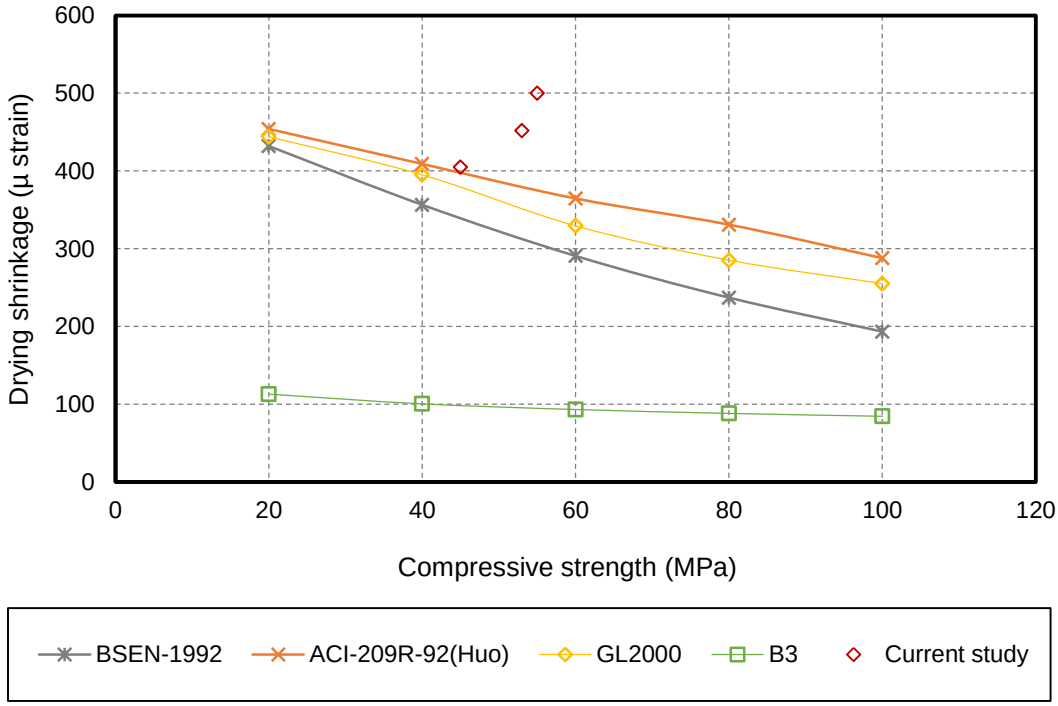

Figure 12 Effect of compressive strength on drying shrinkage strain using different models.

Figure 12 shows the relation between compressive strength and drying shrinkage strain predicted by different models. Compressive strength of concrete is considered as the main parameter for calculating drying shrinkage strain using BSEN-92, ACI 209R-92 (Huo), GL2000 and B3 models. However, it does not considered for calculation drying shrinkage of concrete using ACI

209R-92. From **Figure 12** it can be observed that there was a clear decrease in drying shrinkage strain predicted with the increase of compressive strength using BSEN-92, ACI 209R-92 (Huo) and GL2000 models. Moreover, a small reduction in drying shrinkage strain predicted using the B3 model with the increase in compressive strength was noted. Experimental results of DSSCC obtained from the current study satisfying the range of parameters considered were also plotted to compare with the prediction results as shown in Figure 12. ACI 209R-92 (Huo)'s model shows a close prediction to the experimental results.

5.2 Effect of cement and water content on drying shrinkage using various models

The influence of cement and water content on drying shrinkage is illustrated in **Figure 13** and **Figure 14**. Cement content is considered as one of parameters by ACI 209R-92 and ACI 209R-92 (Huo) to calculate drying shrinkage strain and it does not taken into account as parameter for calculation drying shrinkage by other existing models used in this study. Moreover, the only model of the existing models used that considered water content as one of the parameters to calculate drying shrinkage strain is B3 model. There is an increase in drying shrinkage strain predicted with the increase in cement content using ACI 209R-92 and ACI 209R-92 (Huo) models as shown in **Figure 13.** The increase of water content which was considered as one of the main parameters in the B3 model induces an increase of the drying shrinkage strain predicted as illustrated in **Figure 14.** Some of the experimental results of DSSCC obtained from the current study were plotted in the same figure for comparing with predicted values.

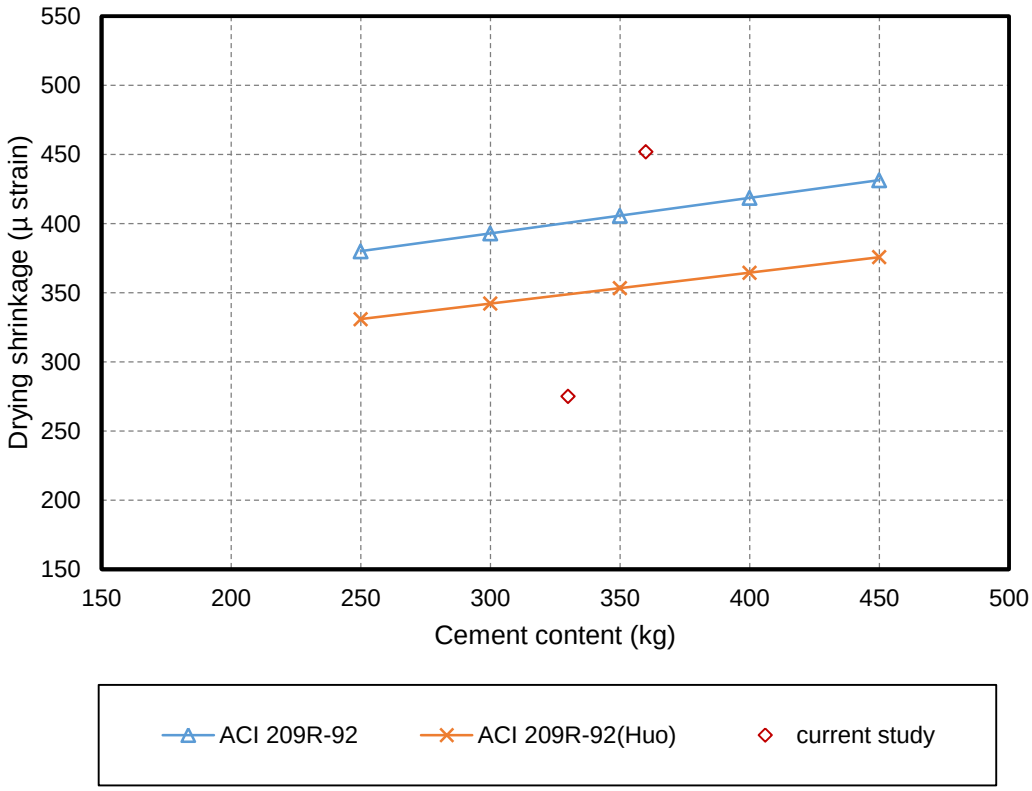

Figure 13 Effect of cement content on drying shrinkage strain for different models.

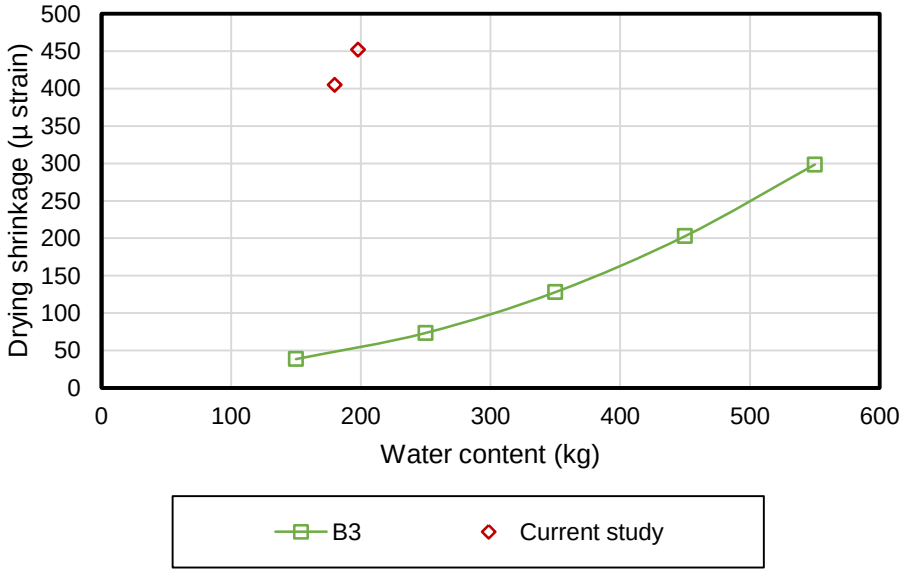

Figure 14 Effect of water content on drying shrinkage using B3 model.

5.3 Effect of relative humidity on drying shrinkage strain using various models

Relative humidity (RH) is one of the more important parameters affecting long term drying shrinkage of concrete. **Figure 15** depicts a clear reduction of drying shrinkage predicted by all models when RH increases. Experimental data of DSSCC obtained from the current investigation were plotted as shown in the same graph. Overall, the predictions obtained from ACI209R-2, GL2000 and ACI209R-92(Huo) are reasonably close to the experimental results.

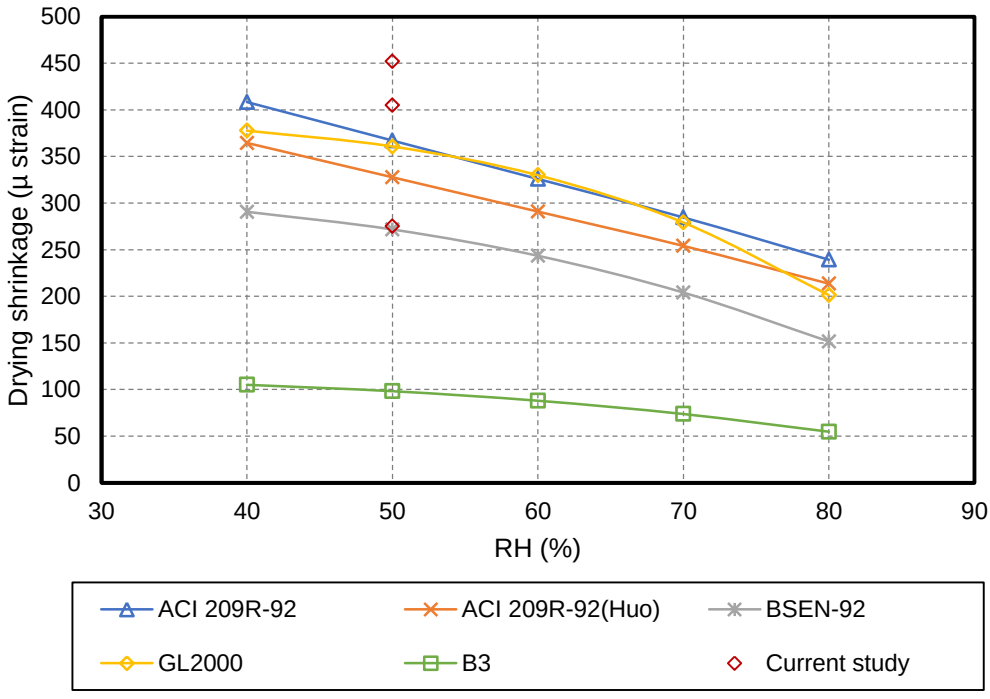

Figure 15 Effect of RH % on drying shrinkage strain using different models.

5.4 Evaluation of existing models using experimental work results

Drying shrinkage strain experimental results obtained in this investigation are compared in **Figure 16** to values calculated by ACI 209R-92, BSEN-92, ACI 209R-92(Huo), B3 and GL2000 models. For each model four statistical observations; mean, standard deviation, coefficient of variation (COV %) and mean absolute error (MAE %) of $\eta = \varepsilon_{Exp}/\varepsilon_{pred}$ were used to compare predictions with experimentally observed drying shrinkage values as summarized in **Table 8.** From **Figure 16** it is observed that the ACI 209R-92, BSEN-92, GL200 and ACI 209R-92(Huo) models have a tendency to overestimate the drying shrinkage values. The B3 model appeared to underestimate drying shrinkage values and resulted in a large scattering compared to other models with the highest mean 1.33 and standard deviation, COV % and MAE% of 0.44, 33.84 and 41.40, respectively. The ACI 209R-92, GL2000 and BSEN-92 models had a mean predicted-to-calculated drying shrinkage ratio of 0.891, 0.847 and 0.823, respectively. However, ACI 209R-92 provided a better prediction of drying shrinkage compared to GL2000 and BSEN-92 with COV% of 9.30% 30% and 37%, respectively. ACI 209R-92 (Huo) was found to overestimate drying shrinkage with a mean of 0.711 and least scatter with a standard deviation of 0.10 and a MAE% equal to 18.40%. The variation values in statistical analysis results (mean, COV and MSE (%)) for all models could be related to the influence of various parameters on the drying shrinkage strain considered for each model.

As mention early in this study the main parameters affecting drying shrinkage strain of SCC are compressive strength, cement content and water to binder ratio. However, each model has different parameters to calculate drying

shrinkage strain. For example compressive strength was considered as main parameters to calculate drying shrinkage strain using ACI 209R-92 (Huo) and GL2000 models, ACI 209R-92 model considers cement content value to calculate drying shrinkage strain. The BSEN-92 and B3 models also consider compressive strength as one of main parameters to calculate drying shrinkage strain. However, both models have taken into their account two parameters as coefficients according to the cement type to calculate drying shrinkage strain.

The experimental work in this study used one type of cement, different cement content and compressive strength obtained were different. This could explain the different in statistical result for the models.

Table 9: Summary of statistical results for drying shrinkage predicted by existing models.

Predictive models	Mean	Standard deviation	COV (%)	MAE (%)
ACI 209R-92	0.891	0.08	9.30	11.4
BSEN-92	0.823	0.30	37.0	29.5
ACI 209R-92(Huo)	0.711	0.10	11.6	18.4
GL2000	0.847	0.26	30	24
B3	1.31	0.44	33.84	41.4

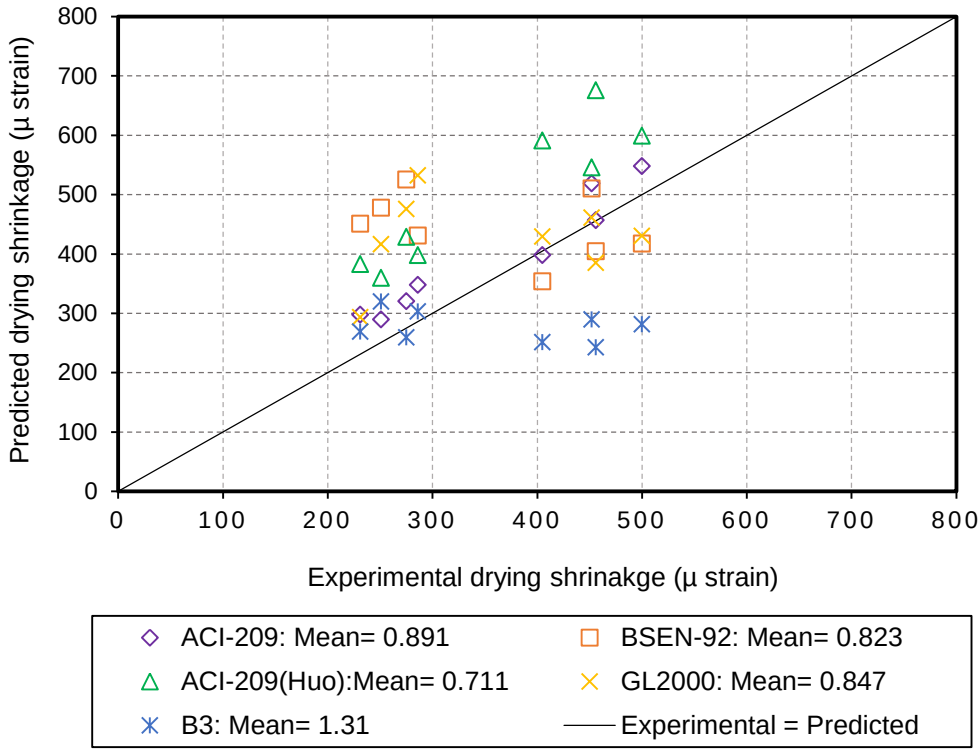

Figure 16 Comparison between experimental and predicted drying shrinkage strains of SCCs using various prediction models

η values were used to indicate the ability of the model to either overestimate or underestimate the drying shrinkage strain of SCC at different age of concrete drying.

$$\eta = \varepsilon_{Exp} / \varepsilon_{Pred} \qquad (2)$$

where ε_{Exp} is the experimental value and ε_{Pred} is the predicted value.

The η values of SCCs for the different predictive models at different ages are plotted in **Figure 17** to **Figure 21.** η values under 1 indicate that a particular model overestimates the drying shrinkage strains and residual values above 1 indicate that the model underestimates them. The best model predicts drying shrinkage when η are closely centred about the one axis and equally distributed

under and above one axis. In this study, the η are plotted against the log time from 4 to 1000 days as well as distribution of the η for all SCCs as percentage (%) are illustrated in the same figures. From **Figure 17** to **Figure 21** it can be observed that the ACI 209R-92, BSEN-92, ACI 209R-92 (Huo) and GL2000 models overestimate most of the drying shrinkage values while the B3 model significantly underestimated the values and resulted in a larger scattering compared to the other models. The results of residual analysis of the models confirmed that the ACI 209R-92, BSEN-92, ACI 209R-92(Huo) and GL2000 models provided overestimations with η distributions of 72%, 59%, 80% and 84% respectively. The BS model produced the lowest predicted drying shrinkage values compared to the experimental results with underestimations of η distributions 80%.

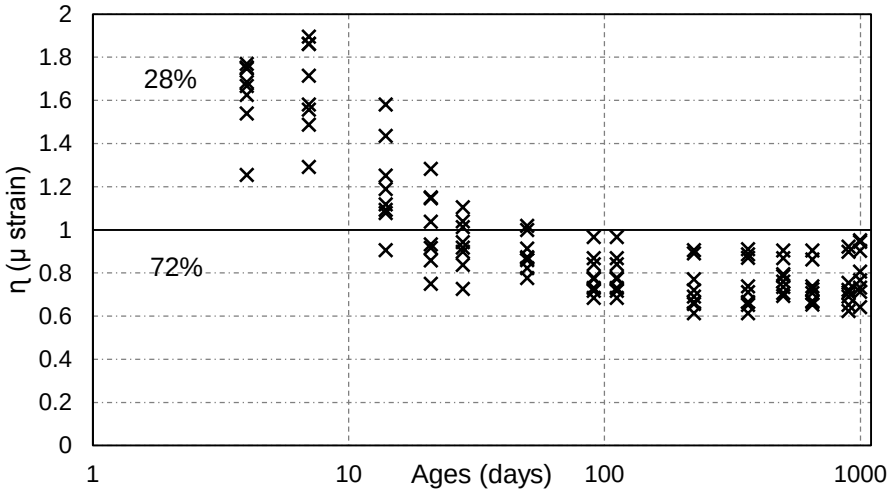

Figure 17 Experimental- to- Predicted values of SCC mixes against ages for ACI 209R-92 model

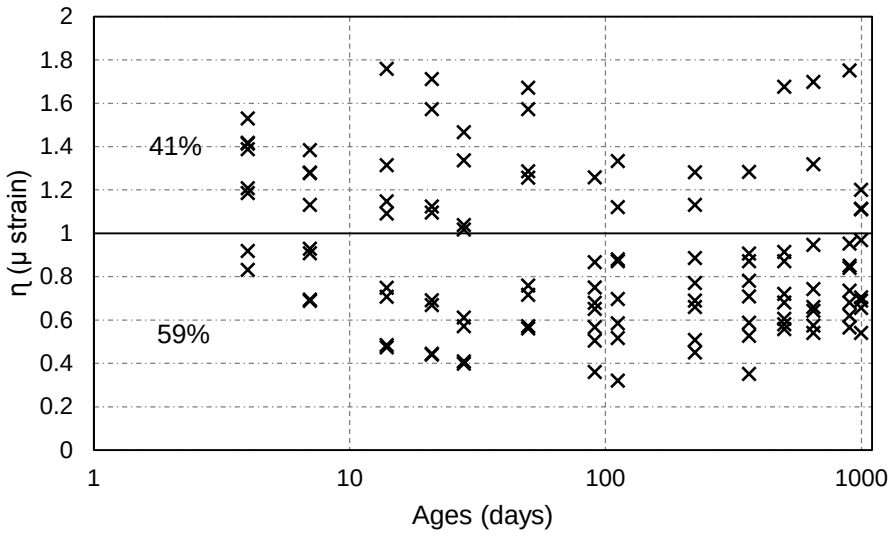

Figure 18 Experimental- to- Predicted values of SCC mixes against ages for BSEN-92 model.

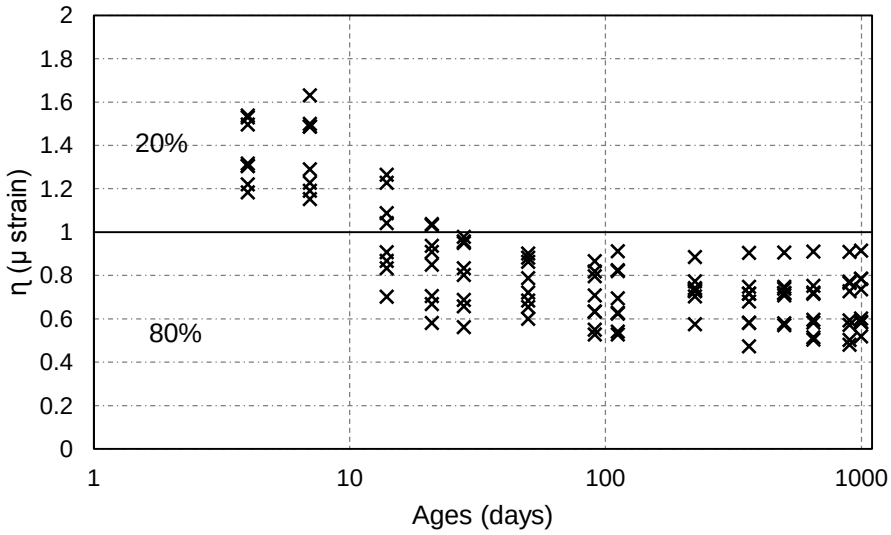

Figure 19 Experimental- to- Predicted values of SCC mixes against ages for ACI 209R-92(Huo) model.

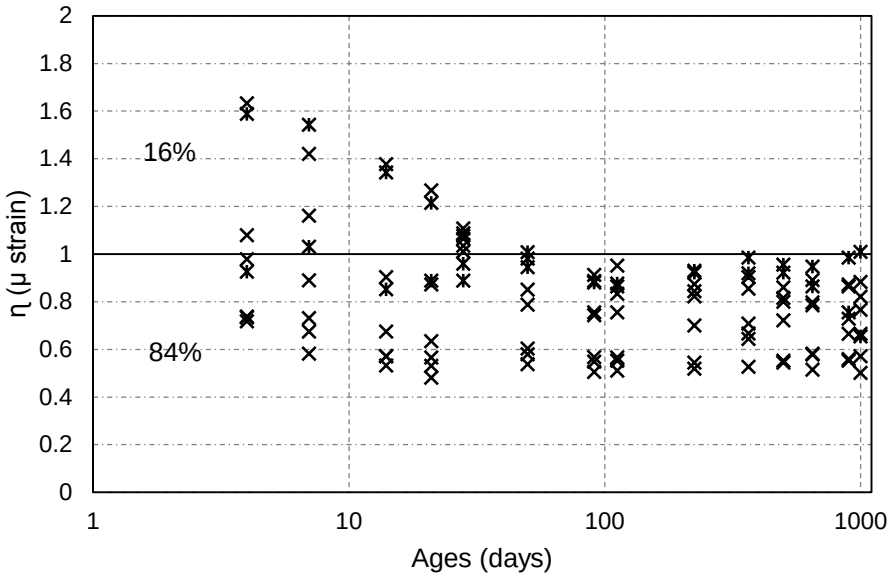

Figure 20 Experimental- to- Predicted values of SCC mixes against ages for GL2000 model.

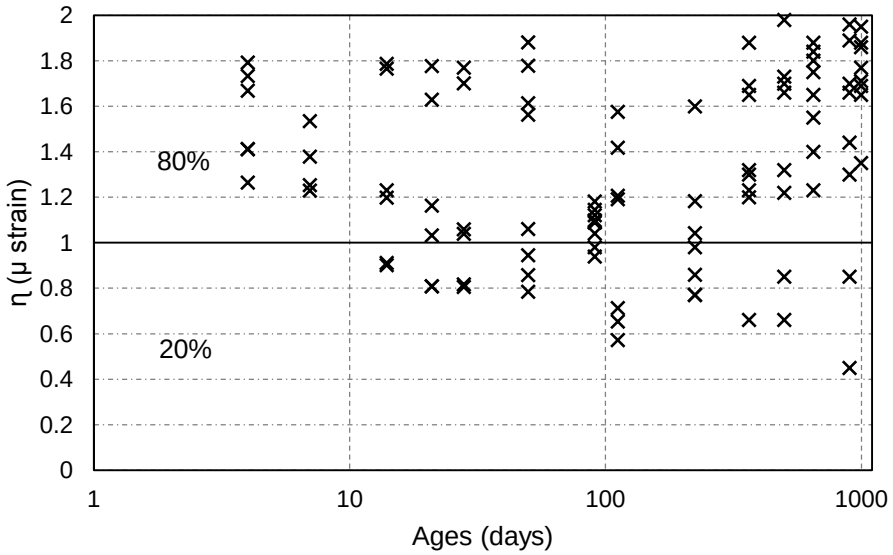

Figure 21 Experimental- to- Predicted values of SCC mixes against ages for B3 model.

It could be concluded that most of the models that were shown, overestimated the values but provided good predictions. However the ACI 209R-92 model exhibited the best estimate of drying shrinkage of SCCs among other models with the lowest MAE of 11.4% and the least scatter with a standard deviation of 0.083.

6 Conclusions

Based on the test results of the experimental program and computational work for comparison between five drying shrinkage models in this investigation, the following conclusions can be highlighted:

1. The addition of fly ash can significantly improve the fresh properties of SCC. The higher the percentage of fly ash, the higher the workability of SCC. Viscosity, passing ability, filling ability and segregation resistance were accepted within the limits required.
2. The compressive strength and flexural strength decreased with the increase of fly ash content due to the lack of lime content. SCCs without fly ash gave the highest value of compressive and flexural strength at 7, 28 and 91 days of age. Using up to 60% of FA as cement replacement can produce SCC with a compressive strength as high as 30 MPa.
3. Water absorption of SCCs is considerably increased when FA was used. However, bulk density of SCCs showed a systematic reduction with increase of FA content for all SCCs. All SCCs and NCs mixes having w/b ratios 0.33 showed lower water absorption than those made with w/b ratios 0.44.
4. SCCs exhibited 5 to 10 % higher drying shrinkage compared with NCs made with a similar w/b ratio up to an age of 91 days. SCC long-term drying shrinkage from 356 to 1000 days was higher than NCs.
5. FA reduced the rate of hydration and thus the drying shrinkage of SCCs containing FA was considerably lower than that of the control concrete.
6. Most of the models used in this study tend to have overestimating characteristics.

7. GL2000 and BSEN-92 models overestimate the drying shrinkage of SCCs. However, the coefficient of variation and the mean absolute error of these models are higher at 30% and 37%, respectively and the mean absolute error for both models are considerably higher.
8. ACI 209R-92 provided a better predicted of drying shrinkage compared to the other models with the lowest coefficient of variation and mean absolute error of 9.5 % and 11.40%, respectively. Moreover, ACI 209R-92-(Huo) model exhibited a good drying shrinkage prediction compared to BSEN-92, GL2000 and B3 models with a lower mean absolute error.
9. The B3 model strongly appeared to underestimate the drying shrinkage strain and resulted in a larger scattering compared to the other models with the highest mean of 1.33.
10. The existing models used in this investigation have considered different parameters to calculate drying shrinkage strain of SCC. This could explain the different in the models accuracy and statistical result for each model

Acknowledgement

The first author would like to acknowledge the financial support of Higher Education of Libya (469/2009).

References

ASSIÉ, S., ESCADEILLAS, G. & WALLER, V. 2007. Estimates of self-compacting concrete 'potential' durability. *Construction and Building Materials,* 21**,** 1909-1917.

BHIRUD, Y. L. & SANGLE, K. K. 2017. Comparison of Shrinkage, Creep and Elastic Shortening of VMA and Powder Type Self-Compacting Concrete and Normal Vibrated Concrete. *Open Journal of Civil Engineering,* 7**,** 130.

BIBM, C. & ERMCO, E. 2005. EFNARC (2005) The European guidelines for self-compacting concrete.
BOUZOUBAA, N. & LACHEMI, M. 2001. Self-compacting concrete incorporating high volumes of class F fly ash: Preliminary results. *Cement and concrete research,* 31**,** 413-420.
CHAN, Y.-W., CHEN, Y.-G. & LIU, Y.-S. 2003. Effect of consolidation on bond of reinforcement in concrete of different workabilities. *ACI Materials Journal,* 100**,** 294-301.
CHOPIN, D., FRANCY, O., LEBOURGEOIS, S. & ROUGEAU, P. Creep and shrinkage of heat-cured self-compacting concrete (SCC). 3rd International Symposium on Self-Compacting Concrete, Reykjavik, Iceland, 2003. 672-683.
COLLEPARDI, M., BORSOI, A., COLLEPARDI, S. & TROLI, R. Strength, shrinkage and creep of SCC and flowing concrete. Second North American Conference on the Design and Use of Self-Consolidating Concrete and the Fourth International RILEM Symposium on Self-Compacting Concrete, 2005. 911-920.
ESQUINAS, A., MOTOS-PÉREZ, D., JIMÉNEZ, M., RAMOS, C., JIMÉNEZ, J. & FERNÁNDEZ, J. 2018. Mechanical and durability behaviour of self-compacting concretes for application in the manufacture of hazardous waste containers. *Construction and Building Materials,* 168**,** 442-458.
FELEKOGLU, B. 2007. Utilisation of high volumes of limestone quarry wastes in concrete industry (self-compacting concrete case). *Resources, Conservation and Recycling,* 51**,** 770-791.
FERNANDEZ-GOMEZ, J. & LANDSBERGER, G. A. 2007. Evaluation of shrinkage prediction models for self-consolidating concrete. *ACI Materials Journal,* 104.
HEIRMAN, G. & VANDEWALLE, L. The influence of fillers on the properties of self-compacting concrete in fresh and hardened state. Proc. of the 3rd Int. Symp. on Self-Compacting Concrete (SCC2003), 2003. RILEM Publications SARL, 606-618.
HEIRMAN, G., VANDEWALLE, L. & VAN GEMERT, D. Influence of mineral additions and chemical admixtures on setting and volumetric autogenous shrinkage of SCC-equivalent mortars. Proc. of the 5th Int. RILEM Symp. on Self-Compacting Concrete (SCC2007), 2007. 553-558.
HUYNH, T.-P., HWANG, C.-L. & LIMONGAN, A. H. 2018. The long-term creep and shrinkage behaviors of green concrete designed for bridge girder using a densified mixture design algorithm. *Cement and Concrete Composites,* 87**,** 79-88.
IQBAL, S., AHSAN, A., HOLSCHEMACHER, K., RIBAKOV, Y. & BIER, T. A. 2017. Effect of Fly Ash on Properties of Self-Compacting High Strength Lightweight Concrete. *Periodica Polytechnica. Civil Engineering,* 61**,** 81.
ISMAIL, I., BERNAL, S. A., PROVIS, J. L., SAN NICOLAS, R., HAMDAN, S. & VAN DEVENTER, J. S. 2014. Modification of phase evolution in alkali-activated blast furnace slag by the incorporation of fly ash. *Cement and Concrete Composites,* 45**,** 125-135.
KHATIB, J. 2008. Performance of self-compacting concrete containing fly ash. *Construction and Building Materials,* 22**,** 1963-1971.
KHATIB, J. M. 2005. Properties of concrete incorporating fine recycled aggregate. *Cement and concrete research,* 35**,** 763-769.

KIM, J.-K., HAN, S. H., PARK, Y. D. & NOH, J. H. 1998. Material properties of self-flowing concrete. *Journal of Materials in Civil Engineering,* 10**,** 244-249.

KLUG, Y. & HOLSCHEMACHER, K. Comparison of the hardened properties of self-compacting and normal vibrated concrete. 3rd RILEM Symposium on Self Compacting Concrete, Reykjavik, 2003 Bagneux, France. RILEM, 596-605.

LOSER, R. & LEEMANN, A. 2009. Shrinkage and restrained shrinkage cracking of self-compacting concrete compared to conventionally vibrated concrete. *Materials and structures,* 42**,** 71-82.

NAGATAKI, S. & FUJIWARA, H. 1995. Self-compacting property of highly flowable concrete. *Special Publication,* 154**,** 301-314.

OKAMURA, H. & OUCHI, M. 2003. Self-compacting concrete. *Journal of advanced concrete technology,* 1**,** 5-15.

PERSSON, B. 2001. A comparison between mechanical properties of self-compacting concrete and the corresponding properties of normal concrete. *Cement and concrete Research,* 31**,** 193-198.

PIERARD, J., DIERYCK, V. & DESMYTER, J. Autogeneous Shrinkage of Self-Compacting Concrete. Second North American Conference on the Design and Use of Self-Consolidating Concrete and the Fourth International RILEM Symposium on Self-Compacting Concrete, 2005. 1013-1022.

PONS, G., PROUST, E. & ASSIÉ, S. Creep and shrinkage of self-compacting concrete: a different behaviour compared with vibrated concrete. Proceedings of the 3rd International RILEM Symposium on Self-Compacting Concrete, 2003. 17-20.

POPPE, A.-M. & DE SCHUTTER, G. Creep and shrinkage of self-compacting concrete. First International Symposium on Design, Performance and Use of Self-Consolidating Concrete, China, 2005. 329-336.

PROUST, E. & PONS, G. 2001. Macroscopic and microscopic behavior of self-compacting concrete creep and shrinkage. *Proc. of Concreep,* 6**,** 569-574.

ROLS, S., AMBROISE, J. & PERA, J. 1999. Effects of different viscosity agents on the properties of self-leveling concrete. *Cement and Concrete Research,* 29**,** 261-266.

SAHA, A. K. & SARKER, P. K. 2017. Sustainable use of ferronickel slag fine aggregate and fly ash in structural concrete: Mechanical properties and leaching study. *Journal of Cleaner Production,* 162**,** 438-448.

SENG, V. & SHIMA, H. Creep and shrinkage of self-compacting concrete with different limestone powder contents. Second North American Conference on the Design and Use of Self-Consolidating Concrete and the Fourth International RILEM Symposium on Self-Compacting Concrete, 2005. 981-987.

SIDDIQUE, R. 2004. Performance characteristics of high-volume Class F fly ash concrete. *Cement and Concrete Research,* 34**,** 487-493.

SIDDIQUE, R. 2013. Compressive strength, water absorption, sorptivity, abrasion resistance and permeability of self-compacting concrete containing coal bottom ash. *Construction and Building Materials,* 47**,** 1444-1450.

TURCRY, P. & LOUKILI, A. A study of plastic shrinkage of self-compacting concrete. Proceedings of the 3rd international RILEM symposium on self-compacting concrete. Reykjavik: RILEM Publications SARL, 2003. 576-585.

TURCRY, P., LOUKILI, A., HAIDAR, K., PIJAUDIER-CABOT, G. & BELARBI, A. 2006. Cracking tendency of self-compacting concrete subjected to restrained shrinkage: experimental study and modeling. *Journal of Materials in Civil Engineering,* 18**,** 46-54.

VALCUENDE, M., MARCO, E., PARRA, C. & SERNA, P. 2012. Influence of limestone filler and viscosity-modifying admixture on the shrinkage of self-compacting concrete. *Cement and Concrete Research,* 42**,** 583-592.

VIEIRA, M. & BETTENCOURT, A. Deformability of hardened SCC. International RILEM Symposium on Self-Compacting Concrete, 2003. RILEM Publications SARL, 637-644.